Journal of Statistical Physics, Vol. 33, No. 2, 1983

Structure and Thermodynamics of the Classical One-Component Plasma

H. B. Singh[1]

Received March 15, 1983; revised April 26, 1983

An exact solution of the mean spherical approximation for charged hard spheres in a neutralizing background is used to calculate various static properties of the classical one-component plasma in the strong coupling regime. The expressions involved are simple and analytic, and involve the charged hard sphere diameter as the only unknown parameter, which we determine using an approximate scaling property of the direct correlation function. Results obtained for structural correlation functions and various thermodynamic quantities are in very good agreement with the Monte Carlo simulation data.

KEY WORDS: Mean spherical approximation; classical one-component plasma; charged hard spheres; static correlation functions; internal energy; compressibility.

1. INTRODUCTION

There has been much interest in the study of ionic fluids. The classical one-component plasma (OCP) is probably the simplest such fluid. It is constituted by an active species of identical point charges embedded in an inert neutralizing background. Apart from serving as a useful model[1,2] in the study of astrophysical objects and plasma physics, the OCP and its variations[2] have recently started finding applications in the study of liquid metals, molten salts, and superionic conductors. Because of the scaling property of its interaction potential, the thermodynamic state of an OCP can be characterized by a single-parameter Γ. It denotes the ratio of the average potential to the average kinetic energy, $\Gamma = \beta e^2/a$, for a system of

[1] Fachrichtung Theoretische Physik, Universität des Saarlandes, D-6600 Saarbrücken, Federal Republic of Germany.

0022-4715/83/1100-0371$03.00/0

particles of charge e at the inverse temperature $\beta = (k_B T)^{-1}$ and with an average number density n corresponding to an average ion-sphere radius a (i.e., $n^{-1} = 4\pi a^3/3$). We shall be considering only the static properties of the system in the strong coupling (i.e., $\Gamma \gtrsim 1$) regime.

The interest in this field has been stimulated by exhaustive Monte Carlo[1–6] (MC) and molecular dynamics simulations leading to accurate data for different structural correlation functions and thermodynamic quantities for $1 \lesssim \Gamma \lesssim 180$. To understand these data qualitatively, the hypernetted chain (HNC) equation[7] and the mean spherical approximation[8,9] (MSA) for charged hard spheres have proved to be quite useful. An apparent shortcoming of both methods[7,9] is the large thermodynamic inconsistency, i.e., the isothermal compressibility calculated from the long-wavelength limit of the static structure factor differs significantly (~40% near crystallization) from that calculated by differentiating the equation of state. The thermal energies in both approximations also deviate appreciably (again by about 40% near crystallization) from the Monte Carlo data.[6] Further, the amplitudes of different correlation functions do not agree with the corresponding results from MC simulations.[3–5] Recently MacGowan has improved (however, at the cost of more numerical work) the results of Gillan,[9] firstly[10] using the stationarity property of the Helmholtz free energy, and secondly[11] using the criterion of thermodynamic consistency, to determine the packing fraction η.

In order to overcome the shortcomings in the HNC equation, Rosenfeld and Ashcroft[12] have given its semiempirical modification. They have approximated the contribution of bridge diagrams by a form valid for a hard sphere fluid, whereby the hard sphere diameter (or the packing fraction) is determined by the requirement of thermodynamic consistency. A modification of the MSA has also been recently obtained by Chaturvedi *et al.*[13] They have introduced two new parameters through a term in the direct correlation function to account for the intermediate-range correlations. These parameters are then determined by building in the Monte Carlo equation of state and the thermodynamic consistency. The results of both these attempts[12,13] are very promising but a considerable amount of computational work is still required for their solutions.

The purpose of the present paper is to show that results of comparable quality can be obtained in a much simpler way. This is achieved by using the MSA[8,9] as such so that the direct correlation function $c(r)$ is given by a simple algebraic expression. The only unknown parameter is the charged hard sphere (CHS) diameter σ which is determined using a scaling property of $c(r)$. Results obtained for different correlation functions, internal and thermal energy are in very good agreement with the MC data.[4–6]

2. THE MODEL

The classical one-component plasma is considered[9] a system of charged hard spheres in an inert neutralizing background. It is quite plausible at strong couplings since the CHS diameter may then be interpreted as the diameter of the Coulomb hole around the point particle. This model system has been solved exactly by Palmer and Weeks[8] in a mean spherical approximation. Their result for the direct correlation function, appropriate for an OCP, can be written as

$$c(r) = \begin{cases} A + Br + Cr^2 + Dr^3 + Er^5, & \text{for } r < \lambda \\ -\dfrac{\Gamma}{r}, & \text{for } r > \lambda \end{cases} \tag{1}$$

where $\lambda = \sigma/a$ and r is expressed in units of a. The coefficients in Eq. (1) are given as

$$A = -\frac{(1+2\eta)^2}{(1-\eta)^4} + \frac{Q^2}{4(1-\eta)^2} - \frac{(1+\eta)Q\kappa}{12\eta} - \frac{(5+\eta^2)\kappa^2}{60\eta} \tag{2a}$$

$$B = 3\lambda^2 M^2/4, \qquad C = \Gamma/2 \tag{2b}$$

$$D = \frac{1}{16}\left(A + 2\frac{\beta U}{N}\right), \quad \text{and} \quad E = \Gamma/160 \tag{2c}$$

where $\eta = (\pi/6)n\sigma^3 = (\lambda/2)^3$ and $\kappa = (3\lambda^2\Gamma)^{1/2}$ are the packing fraction and the Debye–Hückel inverse screening length, respectively. Furthermore,

$$Q = \frac{1+2\eta}{1-\eta}\left\{1 - \left[1 + \frac{2(1-\eta)^3\kappa}{(1+2\eta)^2}\right]^{1/2}\right\} \tag{3a}$$

$$M = Q^2/24\eta - (1 + \eta/2)/(1-\eta)^2 \tag{3b}$$

and the excess internal energy U is given by

$$\frac{\beta U}{N} = -\frac{\Gamma}{\lambda}\left[\left(1 + \eta - \frac{\eta^2}{5}\right) + \frac{Q}{\kappa}(1-\eta)\right] \tag{3c}$$

Apart from $c(r)$, other correlation functions of interest are the pair correlation function $g(r)$ and the static structure factor $S(q)$. They are given by

$$S(q) = \frac{1}{1 - \tilde{c}(q)} \tag{4}$$

and

$$g(r) = 1 + \frac{2}{3\pi r}\int_0^\infty dq\, q\big[S(q) - 1\big]\sin(qr) \tag{5}$$

where q is expressed in units of a^{-1}. In addition, $\tilde{c}(q)$ is the Fourier transform of $c(r)$ and is given by

$$\begin{aligned}\tilde{c}(q) = (3\lambda^3/x^6)\big\{ & Ax^3(\sin x - x\cos x) \\ & + B\lambda x^2\big[2x\sin x - (x^2-2)\cos x - 2\big] \\ & + C\lambda^2\big[(3x^2-6)\sin x - (x^2-6)x\cos x\big] \\ & + D\lambda^3\big[(4x^2-24)x\sin x - (x^4 - 12x^2 + 24)\cos x + 24\big] \\ & + E\lambda^5\big[6(x^4 - 20x^2 + 120)x\sin x \\ & \qquad - (x^6 - 30x^4 + 360x^2 - 720)\cos x - 720\big]/x^2 \\ & - (\Gamma x^4/\lambda)\cos x\big\}\end{aligned} \tag{6}$$

where $x = \lambda q$.

In calculating any of the above quantities, only the CHS diameter σ enters as the unknown parameter. It is well known that the hard sphere correlation functions have built in jump discontinuity at the HS boundary. Gillan[9] has determined σ by requiring that the pair correlation function should be continuous at the hard sphere boundary. This requirement can be seen to imply[8] that the coefficient M given by Eq. (3b) vanishes. The value of σ thus obtained shall be denoted by σ_0. Since the results obtained using this choice for σ are not very encouraging, a different track will be followed. It can be seen that for large values of Γ, the direct correlation function is in leading order a linear function of Γ so that $c(r)/\Gamma$ is nearly a scaled quantity. In particular, the Monte Carlo data[2,14] indicate that for $\Gamma \gtrsim 10$, the value of $c(r=0)/\Gamma$ is around -1.33 irrespective of the value of Γ. This is taken as a new criterion to calculate σ, which from Eq. (1) implies that

$$c(r=0) = A = -1.33\Gamma \tag{7}$$

Accordingly the solution to Eq. (7) provides a unique value for σ which we term as σ_P.

It is now straightforward to calculate any of the correlation or thermodynamic functions. The results obtained this way are presented in the next section and are compared with the Monte Carlo data.

3. RESULTS AND DISCUSSION

3.1. Correlation Functions

The results for the direct correlation function for $\Gamma = 80$ and 160 are plotted in Fig. 1. The MC values are due to DeWitt and are taken from Ref. 12. It is seen that the present results (i.e., with $\sigma = \sigma_p$) are in much better agreement with the MC data. A small jump discontinuity[10,11] at the hard sphere boundary is due to the HS nature of the approximation which is not constrained to become zero as is the case[9] with the choice $\sigma = \sigma_0$. In order to verify that $c(r)/\Gamma$ is a scaled function of r, we plot this quantity for $\Gamma = 20$, 40, and 200 in Fig. 2. The three curves lie very close to one

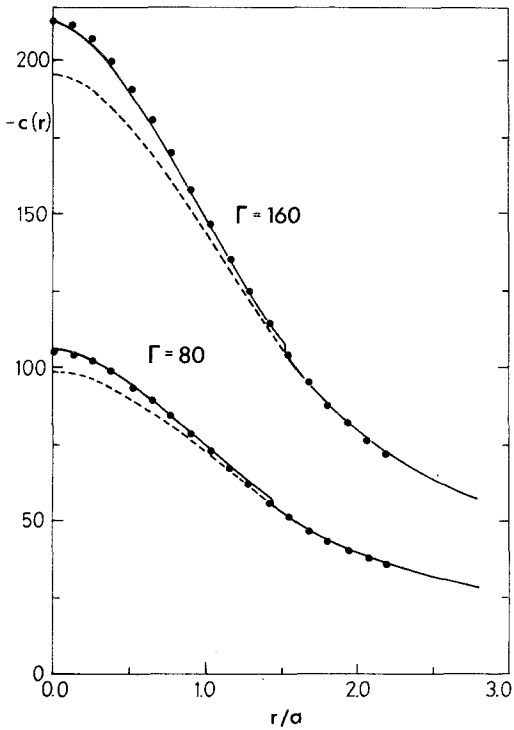

Fig. 1. The direct correlation function $c(r)$ of the OCP for $\Gamma = 80$ and 160. Dashed curve is obtained for the choice $\sigma = \sigma_0$. Full curve represents the present results, i.e., those obtained with the choice $\sigma = \sigma_p$ as given from Eq. (7). The filled circles are the Monte Carlo results of DeWitt and are taken from Ref. 12. (In the figures r and q are expressed in their natural units.)

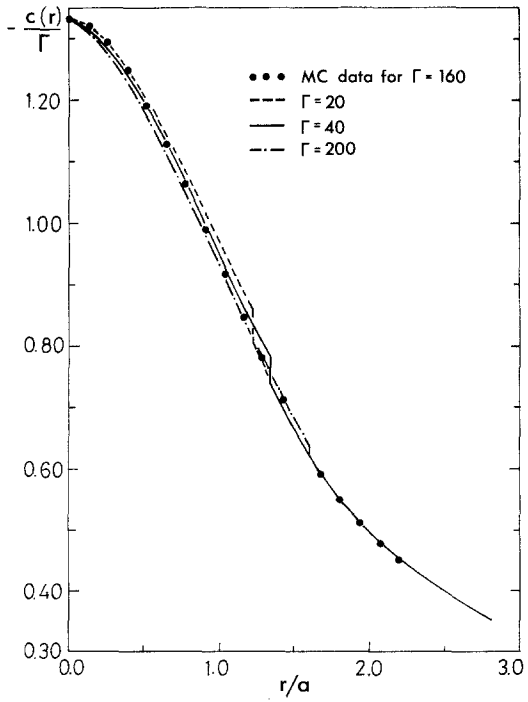

Fig. 2. The present results for $c(r)/\Gamma$ versus r/a for $\Gamma = 20$, 40, and 200. The filled circles represent Monte Carlo results of DeWitt at $\Gamma = 160$.

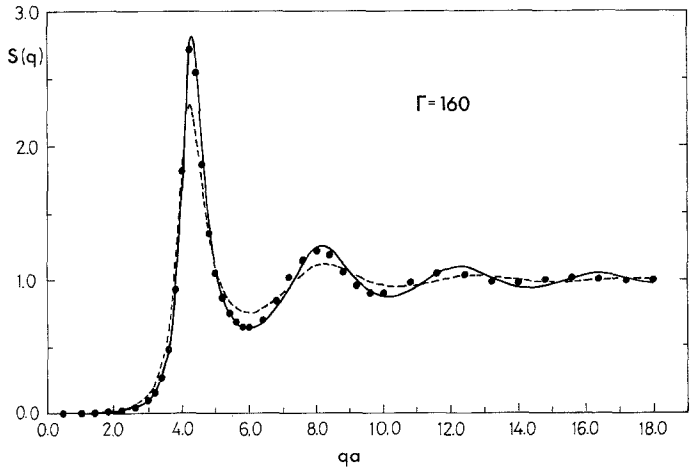

Fig. 3. The OCP static structure factor $S(q)$ versus qa at $\Gamma = 160$. The curves are labeled as in Fig. 1. The Monte Carlo data (filled circles) are due to Galam and Hansen (Ref. 4).

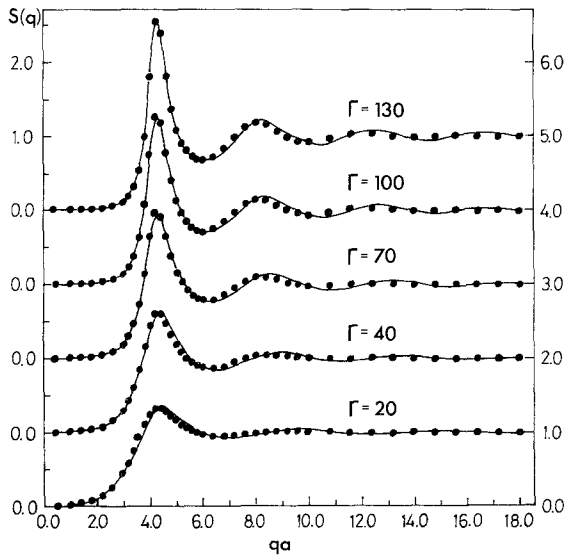

Fig. 4. Here the present results for the static structure factor are plotted at different values of Γ. The filled circles represent the Monte Carlo data of Galam and Hansen (Ref. 4).

another. In fact, the maximal difference between the values of $c(r)/\Gamma$ for $\Gamma = 40$ and 200 is less than 3%. The results for the static structure factor as obtained from Eq. (4) are presented in Figs. 3 and 4, and are compared with the tabulated data of Galam and Hansen.[4] The present results represent a large improvement over the results[9] for $\sigma = \sigma_0$ and also over the results of MacGowan,[10,11] and are in very good agreement with the MC data. For the sake of clarity, the results of $S(q)$ obtained for $\sigma = \sigma_0$ are plotted only in Fig. 1, for $\Gamma = 160$.

The pair correlation function is obtained from Eq. (5) by Fourier transforming $S(q)$. Here we have a convergence problem in the small r region because the dominant term in the large q expansion of $S(q)$ is proportional to the coefficient M which is not zero in the present case. In order to overcome this problem, we take $g(r)$ to be equal to zero in the hard core region—in accordance with the basic assumption of MSA. Its value at the HS boundary is calculated analytically from[8] $g(r = \sigma^+) = -M$. For distances larger than the hard sphere diameter, $g(r)$ is determined from Eq. (5). For that, the integral in Eq. (5) is truncated after $q = 4300$ and the integration interval is divided in 500 parts. Integration in each of these subintervals is done using the Gauss quadrature method with five points. In order to make sure that integration in a subinterval is done correctly, this subinterval is continuously halved until a desired relative accuracy (in the

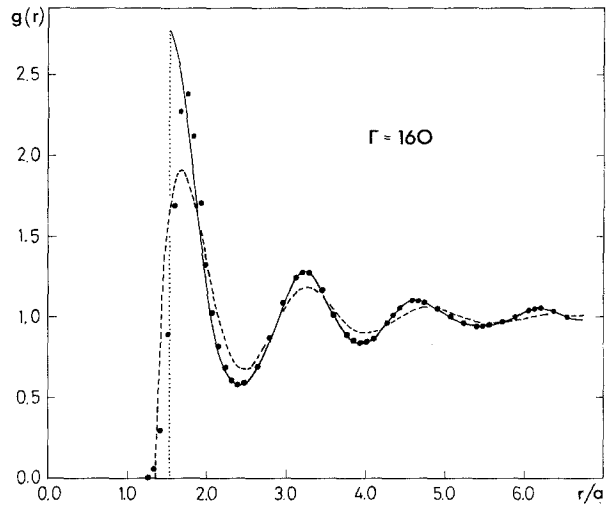

Fig. 5. The OCP pair correlation function $g(r)$ at $\Gamma = 160$. Dashed curve is obtained for $\sigma = \sigma_0$ and the full curve represents the present results (i.e., with $\sigma = \sigma_p$). The dotted line at $r = \sigma_p$ indicates the jump discontinuity in the value of $g(r = \sigma_p)$. The Monte Carlo data (filled circles) are due to Slattery *et al.* (Ref. 5).

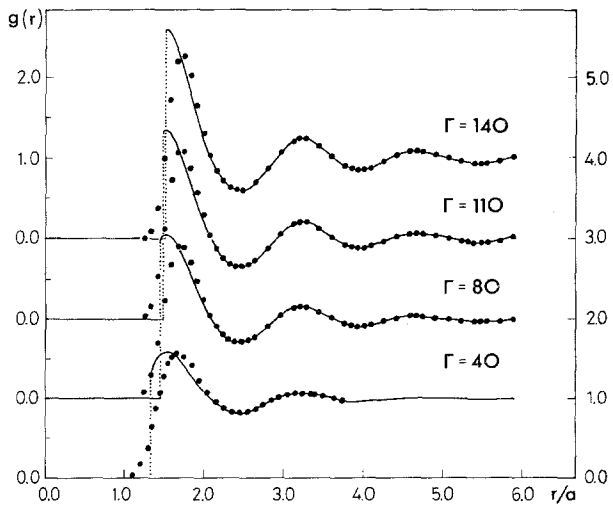

Fig. 6. The present results for the pair correlation function versus r/a at different values of Γ. The dotted line for each Γ indicates the discontinuity in the value of $g(r)$ at the hard sphere boundary. Filled circles for $\Gamma = 80$, 110, and 140 represent the Monte Carlo data of Slattery *et al.* (Ref. 5). The Monte Carlo data at $\Gamma = 40$ are taken from Brush *et al.* as Slattery *et al.* have not given the data for $\Gamma < 80$.

present case 0.10) is reached. Demanding a still better relative accuracy of 0.02 leaves the present results practically unchanged. Further, to check that there is no appreciable truncation error, the upper limit was raised to 6500. The results so obtained differ negligibly from the present results except in the immediate vicinity of the HS boundary ($\sigma^+ < r \lesssim 1.1\sigma$) where the maximum discrepancy between the two is about 5%. The present results for the pair correlation function are plotted in Figs. 5 and 6 and are compared with the tabulated data of Slattery *et al.*[5] As can be seen the agreement with the MC data is excellent beyond the first peak region. The well-known[9–13] discrepancies near the first peak region remain and their origin lies in the hard sphere feature of the approximation. Remember, that the object approximated by a charged hard sphere is in fact a point charged particle surrounded by a spherical empty space in which no other plasma particle is able to penetrate owing to strong Coulomb repulsions. A small overlap of such Coulomb holes is possible in principle which, however, is not allowed in the hard sphere model. This leads naturally to a severe constraint on the behavior of the pair correlation function near the hard sphere boundary. This also seems to be the reason for the failure of MSA and its modification[13] in the small-Γ region, since in this region the Coulomb hole becomes softer and softer owing to reduced Coulomb repulsions. In this region the hypernetted chain equation works[12] quite well.

3.2. Thermodynamics

An important quantity for the calculation of thermodynamic properties of a system is its internal energy. Other thermodynamic quantities like specific heats, compressibility, and thermal expansion coefficients etc. can be easily obtained[2] from it. Presently, the excess internal energy U is calculated from the analytic expression given by Eq. (3c) and the numerical results obtained are given in Table I. For comparison, we list the very recent Monte Carlo data of Slattery *et al.*[6] where they have analyzed the N dependence of the results for U. The MC value of U for a particular Γ given in the table corresponds to the smallest value of N beyond which the numbers for the internal energy become practically N independent. As can be seen, the present results (i.e., with $\sigma = \sigma_p$) are in very good agreement with the MC data. For example, the deviation which at $\Gamma = 80$ is about 0.1%, gradually diminishes to less than 0.01% for $\Gamma = 160$. On the other hand the corresponding deviation for the choice[9] $\sigma = \sigma_0$ is about 0.54% and remains constant with increasing Γ.

It is known[3] that at stronger couplings, the purely static energy U_0 (i.e., the value of the internal energy for a perfect bcc lattice, $\beta U_0/N =$

Table I. The Charged Hard Sphere Diameter σ_p, the Corresponding Packing Fraction η, and the Excess Internal Energy $\beta U/N$ [a]

Γ	σ_p/a	η	$-(\beta U/N)_{\sigma=\sigma_p}$	$-(\beta U/N)_{MC}$	$-(\beta U/N)_{\sigma=\sigma_0}$
10	0.985	0.120	8.053	7.998	8.053
20	1.223	0.229	16.759	16.673	16.667
30	1.300	0.275	25.534	25.439	25.373
40	1.348	0.306	34.349	34.255	34.125
50	1.382	0.330	43.188	43.102	42.907
60	1.408	0.349	52.045	51.956	51.710
70	1.429	0.365	60.915	—	60.529
80	1.446	0.378	69.793	69.725	69.360
90	1.461	0.390	78.683	—	78.202
100	1.473	0.400	87.576	87.524	87.053
110	1.485	0.409	96.479	96.411	95.911
120	1.495	0.418	105.384	105.343	104.775
130	1.504	0.425	114.295	114.264	113.645
140	1.512	0.433	123.211	123.181	122.520
150	1.520	0.439	132.129	132.115	131.399
160	1.527	0.445	141.051	141.039	140.282
170	1.533	0.451	149.976	149.966	149.169
180	1.539	0.456	158.904	—	158.059
200	1.550	0.466	176.762	176.765	175.848

[a] The results for $\beta U/N$ for $\sigma = \sigma_0$ and $\sigma = \sigma_p$ are compared with the recent (Ref. 6) Monte Carlo data.

-0.895929Γ) accounts for most of the internal energy. Thus it is very important to know the thermal fraction of the energy,

$$\beta \frac{\Delta U}{N} = \frac{\beta}{N}(U - U_0) \tag{8}$$

very accurately, if the fluid–solid transition is to be located precisely.[2] In Fig. 7, the results for the thermal energy are plotted over the whole range of Γ and are compared with the MC data.[6] Obviously, the small differences in the internal energies become very prominent. Accordingly it can be seen that the present results are in good agreement with the data, whereas deviations for the case $\sigma = \sigma_0$ are very large and are monotonically increasing with Γ.

[2] The latest value of Γ at which the fluid–solid transition takes place has been estimated to be 178 ± 1, by Slattery *et al.* using their most recent data (Ref. 6) on internal energies.

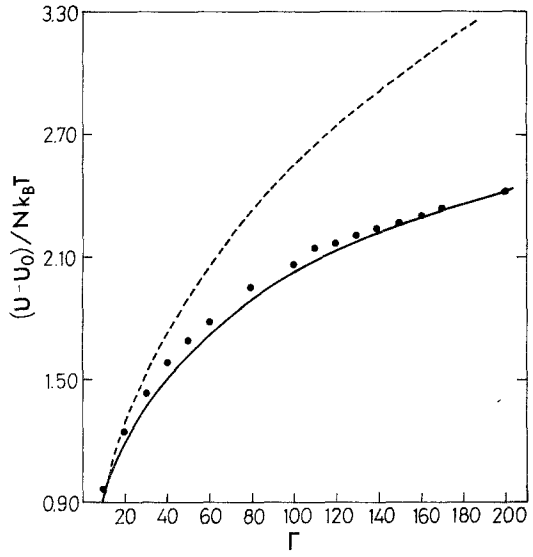

Fig. 7. Thermal energy $(U - U_0)/Nk_BT$ of the OCP versus Γ. Dashed curve is obtained for $\sigma = \sigma_0$ and the full curve represents the present results. The filled circles denote the recent (Ref. 6) Monte Carlo results of Slattery *et al.*

The only other thermodynamic quantity in which we are interested is the isothermal compressibility[15] χ, which can be calculated in two ways—the difference in the two values being the measure of thermodynamic inconsistency. One way to calculate χ proceeds from the equation of state, i.e.,

$$\frac{\chi_0}{\chi} = 1 + \frac{\beta U}{3N} + \frac{\Gamma}{9}\frac{\partial}{\partial \Gamma}\left(\frac{\beta U}{N}\right) \tag{9}$$

where $\chi_0 = \beta/n$ is the ideal gas isothermal compressibility. The second way to calculate χ is[15] via the long-wavelength limit of structural correlation functions, e.g.,

$$\frac{\chi_0}{\chi} = \lim_{q \to 0}\left[\frac{1}{S(q)} - \frac{\kappa^2}{\lambda^2 q^2}\right] \tag{10}$$

so that

$$\frac{\chi_0}{\chi} = 1 - 3\lambda^3\left(\frac{A}{3} + \frac{B\lambda}{4} + \frac{C\lambda^2}{5} + \frac{D\lambda^3}{6} + \frac{E\lambda^5}{8} + \frac{\Gamma}{2\lambda}\right) \tag{11}$$

The results obtained for the inverse compressibility from Eqs. (9) and (11) are plotted in Fig. 8 and are compared with the Monte Carlo data taken

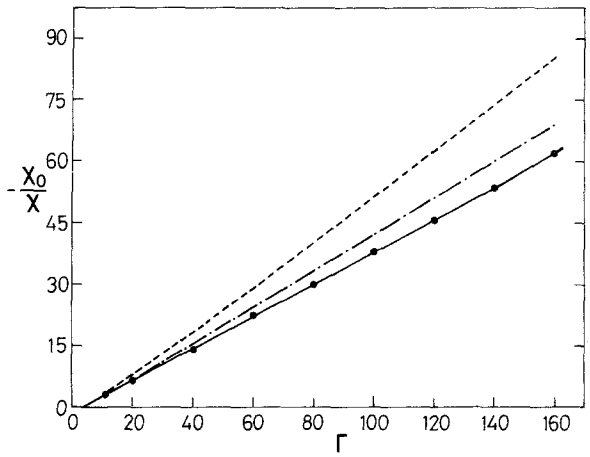

Fig. 8. The OCP inverse compressibility χ_0/χ versus Γ. Dashed curve denotes the results obtained from Eq. (11) with the choice $\sigma = \sigma_0$. The dashed–dotted curve represents the corresponding results with the choice $\sigma = \sigma_p$. The full curve shows the results for χ_0/χ as obtained from Eq. (9), with the choice $\sigma = \sigma_p$. The filled circles denote the Monte Carlo results taken from Ref. 12.

from Ref. 12. The results for the virial compressibility [i.e., those computed from Eq. (9)] calculated with $\sigma = \sigma_p$ are not distinguishable from the MC data. The other two curves in Fig. 8 show the results for χ_0/χ as obtained from Eq. (11) using $\sigma = \sigma_0$ and $\sigma = \sigma_p$. It is reassuring to note that the thermodynamic inconsistency in the present case has diminished by more than a factor of 3 from the $\sigma = \sigma_0$ case.

Interestingly, our values for the packing fraction η (listed in Table I) are quite close (especially for larger Γ) to those obtained by Rosenfeld and Ashcroft[12] from the hard sphere bridge functions (in the modified HNC equation), which fit the Monte Carlo data for $g(r)$ best. For example, the deviation between the two around $\Gamma = 80$ is about 6% which gradually disappears around $\Gamma = 160$. Also the thermodynamic inconsistency which in both approaches is small, is about the same around $\Gamma = 160$.

4. CONCLUDING REMARKS

It is shown that the simple MSA expression (1) along with the criterion (7) for determining the charged hard sphere diameter, gives results for different static properties of the classical one-component plasma, which are in very good agreement with the Monte Carlo data. The only problem seems to be the region around the hard sphere boundary. While the mean spherical approximation, e.g., constrains $g(r)$ to vanish abruptly at the HS

boundary, the Coulomb holes around point plasma particles have some scope of penetration.

Recently,[16] we have applied this mean spherical approximation with very good success to calculate the static structure factor of liquid alkali metals. σ was, however, determined from a point fit using the experimental data at the first minimum of $S(q)$. We proposed there but did not take into account the effect of small charge polarization of alkali ions. We feel that if that is done and σ is simply determined from Eq. (7), then results of the same quality as obtained earlier[16] can be obtained.

ACKNOWLEDGMENTS

I am thankful to Professor Arno Holz for useful discussions and to Professor J. L. Lebowitz for sending me the reprints of Dr. MacGowan's work. Thanks are also due to Mr. Jörg Kremer for familiarizing me with the Plotter. This work is supported by Deutsche Forschungsgemeinschaft within Sonderforschungsbereich 130.

REFERENCES

1. S. G. Brush, H. L. Sahlin, and E. Teller, *J. Chem. Phys.* **45**:2102 (1966).
2. M. Baus and J. P. Hansen, *Phys. Rep.* **59**:1 (1980).
3. J. P. Hansen, *Phys. Rev. A* **8**:3096 (1973).
4. S. Galam and J. P. Hansen, *Phys. Rev. A* **14**:816 (1976).
5. W. L. Slattery, G. D. Doolen, and H. E. DeWitt, *Phys. Rev. A* **21**:2087 (1980).
6. W. L. Slattery, G. D. Doolen, and H. E. DeWitt, *Phys. Rev. A* **26**:2255 (1982).
7. J. F. Springer, M. A. Pokrant, and F. A. Stevens, Jr., *J. Chem. Phys.* **58**:4863 (1973); K. C. Ng, *J. Chem. Phys.* **61**:2680 (1974).
8. R. G. Palmer and J. D. Weeks, *J. Chem. Phys.* **58**:4171 (1973); H. Gould, R. G. Palmer, and G. A. Estévez, *J. Stat. Phys.* **21**:55 (1979).
9. M. J. Gillan, *J. Phys. C* 7:L1 (1974).
10. D. MacGowan, *J. Phys. C* **16**:59 (1983); *J. Phys. C* **16**:L7 (1983).
11. D. MacGowan, preprint.
12. Y. Rosenfeld and N. W. Ashcroft, *Phys. Rev. A* **20**:1208 (1979).
13. D. K. Chaturvedi, G. Senatore, and M. P. Tosi, *Nuovo Cimento B* **62**:375 (1981); D. K. Chaturvedi, M. Rovere, G. Senatore, and M. P. Tosi, *Physica B* **111**:11 (1981).
14. N. Itoh and S. Ichimaru, *Phys. Rev. A* **16**:2178 (1977).
15. M. Baus, *J. Phys. A* **11**:2451 (1978).
16. H. B. Singh and A. Holz, *Phys. Rev. A* **28**:1108 (1983).